Jour. Geol. Soc. India (2022) 98:1466-1474
https://doi.org/10.1007/s12594-022-2194-8

ORIGINAL ARTICLE

Multithematic Geoscience Data Integration for Identification of Mineral Potential Areas in Parts of Central Indian Precambrian Craton

Ajit Singh*, Debasmita Dash, Rajesh Kumar and Niroj Kumar Sarkar
Remote Sensing Division, RSAS, Geological Survey of India, Kumaraswamy Layout, Bangalore - 560 111, India
***E-mail:** ajitpetro.singh@gmail.com*

Received: 25 June 2021/ Revised form Accepted: 16 October 2021

ABSTRACT

The paper highlights the results of multi-thematic geoscience data integration involving geological, geophysical, geochemical and remote sensing data sets, for an area of 4000 Sq. Km in parts of Precambrian Bastar craton, Chhattisgarh. The present team has been able to identify two discrete mineral potential areas for base metal sulphides, Sn, W and REE in sheared and altered felsic volcanics in Kotra-Bhansula area and for gold in propylitically altered meta basalts in Bhursatola-Khampura area. The dataset utilized during collation and integration includes (i) high resolution aeromagnetic data (ii) 1:50000 geological data covering litho-structural and mineralisation attributes (iii) 1:50 k geochemical data for 61 elements (iv) multispectral ASTER satellite data and its derivative alteration maps. Thematic data and derivative maps were studied and interpreted for evaluation of concerned parameters for estimating their role in mineralisation. The data integration has been implemented in three steps beginning with GIS based spatial modelling using Fuzzy logic method resulting into production of mineral favourability map, followed by detailed field evaluation and characterization of the identified mineral favourability areas. Eventual identification of potential areas was based on synthesis of modelling output, field outcome and laboratory results of analyses carried out on critical samples collected from mineral favourability areas. The identified two mineral potential areas are recommended for further detailed exploration for gold, base metal, Sn, W and REE through surface and sub-surface probing.

INTRODUCTION

Multithematic geoscience data integration in recent times has created a niche for itself in the arena of mineral exploration by discovering new potential zones of mineralization through increased success possibilities, reduced time and risk, improved geological interpretation and development of a suitable concept based mineral model. It results in significant degree of scaling down of target area resulting into minimisation of time and effort during the field work which is the main criterion for utilising these methods. Geo-science data integration in general utilises two different approaches i.e. (i) knowledge driven approach and (ii) data driven approach depending on the types for assigning weights to each evidence layer (Pan et.al 2000, Feltrin, 2008 and Carranza, 2009). The knowledge-driven approach qualitatively evaluates patterns in data and relationship between each evidence layer and the deposits sought and is suited in relatively less explored areas (Bonham-Carter, 1994). Experts opinion plays a significant role in decision making and evaluating relative importance of evidence layers in a knowledge based approach. In contrast, the data-driven method analyses and quantifies the spatial correlation between each evidential layer and the deposit locations of common genesis. The data driven approach in general is well applicable for well-explored areas (Carranza et. al 2008). Applicability of a method relies on availability of information in respect of data density, completeness, quality, and complexity, as well as the level of a priori geological knowledge of an area at local to regional scales (Dubois et al. 1999; Porwal et al. 2003). Due to low exploration data density in the study area, a knowledge-driven methods has been selected for mineral favourability mapping. The current exercise carried out by us is an attempt to evaluate and utilise the newly acquired high resolution aero-magnetic and aero-radiometric data (80m elevation with 300m line spacing) in parts of central Indian craton i.e. Rajnandgaon district, Chhattisgarh in conjunction with legacy geo-science data and to integrate the same using knowledge based integration technique for decrypting potential areas for mineralisation.

REGIONAL GEOLOGY

The study area forms part of the Kotri- Dongargarh Orogen in the Precambrian of central India, Bastar craton (Fig.1). The Bastar craton of central India is an important protocontinental nuclei of the global Archaean record (Bleeker, 2003; Naqvi, 2005). It is flanked by the ENE-WSW trending Central Indian Tectonic Zone (CITZ) towards the north, and is cross cut by the N-S to NNE-SSW trending Kotri lineament that geographically corresponds to a collage of Archaean/ Palaeoproterozoic supracrustal belts; collectively termed the Kotri-Dongargarh mobile belt (KDMB) (Ramakrishnan and Vaidyanadhan, 2010). The KDMB exposes highly tectonised and metamorphosed granite gneiss and metasedimentary association of Bengpal Group which shows characters of Archean high grade gneissic complex. The Lower Proterozoic Bailadila Group forms the lowermost stratigraphic sequence over the basement gneisses and is folded and metamorphosed from greenschist to lower amphibolite facies. The lithounits of Bailadila Group are intruded by sub-volcanic igneous suites and overlain by volcano-sedimentary sequence of Kotri Supergroup in south and by Dongargarh Supergroup of rocks in the north. Kotri Supergroup comprises volcano-sedimentary association represented by Ainhur Group, which is invaded by epizonal multi-phase granitoids known as Bundel granite in the south and is covered by younger sequence of Abujhmar Group. The Dongargarh Supergroup which comprises of bimodal volcanics is the dominant litho assemblage resting unconformably on the Archean gneissic complex, the Amgaon gneisses.

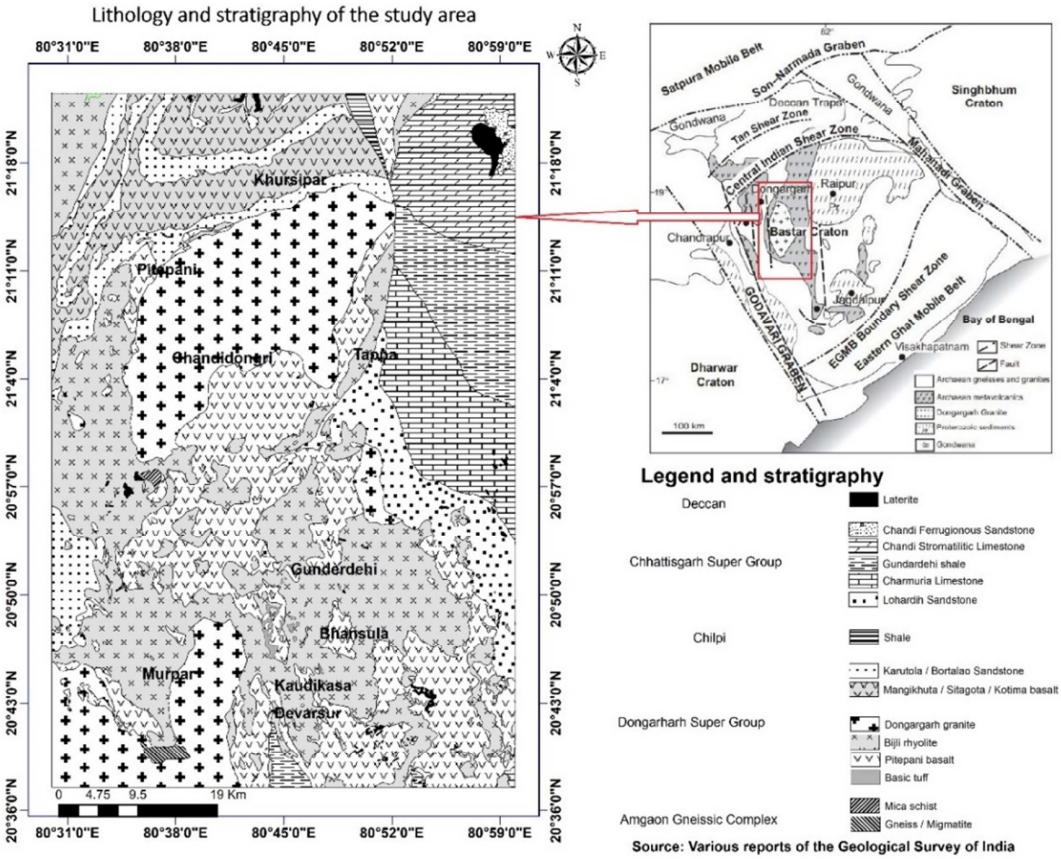

Fig.1. Geological map and stratigraphy of the study area (after Sarkar, 1957-58).

The Dongargarh succession comprises of volcano sedimentary rocks divisible into two groups - The Nandgaon Group comprising of bimodal volcanics and the Khairagarh Group comprising of arkosic and arenite quartzite interbedded with basalts. Early volcanism in the Dongargarh domain is dominated by rhyolite and tuffs (Bijli Formation) followed by lavas of basalt and andesite (Pitepani Formation). The Bijli Rhyolite of the Nandgaon Group gives Rb-Sr whole rock isochron age of 2180±25 Ma (Sarkar, 1958, 1994) and 2503 ± 35 Ma (Krishnamurthy, 1990). The Dongargarh granites have intruded into the Amgaon gneisses and the bimodal volcanic suite of Nandgaon Group. The Dongargarh granites are unconformably overlain by the Khairagarh Group. The U-Pb zircon age of Dongargarh granites is 2432 ± 6 Ma (Ahmad et al., 2008). The Palaeoproterozoic (2.2–2.5 Ga) Dongargarh Group is weakly folded into a synclinal structure (Sitagota syncline), and is intruded by a post-tectonic granite pluton (Dongargarh granite) (Sarkar, 1957–58; Sensarma and Mukhopadhyay, 2003). The Dongargarh Group of rocks is affected by low-grade green-schist facies metamorphism. The geological map of the area is presented in Fig.1 (Sarkar, 1957-58)

DATA ACQUISITION AND METHODOLOGY

Data Acquisition

Geological, aero-geophysical, topographic, remote sensing and geochemical data pertaining to an area of 4000 Sq.Km in the Kotri-Dongargarh belt has been utilised as source evidence for mineral prediction. Geological data were primarily obtained from various field season reports of the Geological Survey of India, on a scale of 1:50,000 or higher which included information on significant litho-tectonic domains, structures such as faults, shear and fracture systems and previously reported incidences of copper, gold, REE and associated mineralisation. Airborne magnetic and radiometric data were acquired using two fixed-wing Pacific Aerospace PAC750 XSTOL aircraft equipped with a magnetic gradiometer system and a gamma ray spectrometer supported by auxiliary instrumentation. The gradiometer system comprised of Geometrics and Scintrex cesium magnetometer sensors installed in wing-tip pods and a tail-boom on the aircraft. Radon corrections were made using a spectral ratio method. Magnetic data was sampled with frequency of 10 Hz, radiometric data with a frequency of 1 Hz. SRTM DEM data has been acquired from USGS earth explorer and is used to map linear topographic highs in the area. Geochemical data utilised in this study is collected from reports of National Geochemical Mapping projects carried out in the central region by the Geological Survey of India and covers roughly 50 % of the area. Although the data package comprises information of a total of 61 elements and 10 major oxides, dispersion pattern of only three elements vis a vis Cu, Pb, Zn have been studied in detail. Mapping of hydrothermal alteration zones has been done by acquiring Landsat-8 and the Advanced Spaceborne Thermal Emission and Reflection Radiometer (ASTER) data which utilise the visible and short infrared region for mapping the distribution and spread of iron oxides, clay minerals as well as phyllic, propylitic and argillic alteration zones.

Methodology

Mineral favourability mapping (MFM) can be represented as generation of a map with higher probability of finding a general and/or specific style of mineral deposits/occurrences as an outcome of GIS based multi-thematic geoscience data integration. GIS based spatial; modelling of geoscience data entails following major steps vis. a vis. (i) creation of a digital data base, (ii) area specific concept development, (iii) creation of evidential maps and (iv) execution of integration operators. Creation of digital data base was carried out by digitising important features from geological maps, derivative aeromagnetic and radiometric maps, geochemical anomalies and

alteration zones obtained from multispectral remote sensing data. Evaluation of individual geo-science data sets with respect to their significance in already existing mineralisation covers the second step i.e. area specific concept building. Based on the knowledge of the particular geological domain attained through literature consultation, discussion with previous workers, etc. scores are assigned to each set of features and evidential thematic maps are created, thus concluding the third step. Execution of integration in GIS platform and subsequent ground evaluation of delineated zones to validate the utility and confidence constitute the fourth and final step.

Fuzzy Logic

Fuzzy logic is a technique based on Fuzzy set theory proposed by Zadeh, 1965 which assists geoscientists in building mineral potential model by selection of evidential layers which are most crucial for a particular style of mineralisation. In classical set theory, the membership of a set is defined as true (=1) or false (=0), whereas the fuzzy-set theory defines a degree of membership in a set, represented by a value between 0 and 1 without a clear and distinct boundary. The fuzzy model for mineral prediction is defined as a generic model: if X represents the set of evidential layers X_i (i = 1, 2, 3, . . . , n) and the layer has r classes defined as (j = 1, 2, 3, . . . , r), then n fuzzy sets A_i (i = 1, 2, 3, . . . , n) in X are defined by equation

$$A_{ij} = \frac{x_{ij}, \mu_A}{x_{ij}} \; \varepsilon \; X_i \quad , \quad (0 \leq \mu_A \leq 1)$$

where μ_A is the membership value. Using a fuzzy set operator, n fuzzy sets A_i are integrated to form a comprehensive fuzzy set F, expressed by the following equation

$$F = \Sigma_{i=1}^{n} A_i$$

Zadeh (1965) and Zimmermann (1991) have defined a set of operators for fuzzy modelling i.e. fuzzy OR, fuzzy AND, the fuzzy algebraic SUM, the fuzzy algebraic PRODUCT and the fuzzy GAMMA operator.

Generation of Evidence Maps

Continuous evidential layers of favourability were generated using geological, aero-magnetic, radiometric, remote sensing and geochemical as described under. The selection of weightage or scores for each data sets or layers of evidence is done on the basis of subjectively assessed favourability for each layer and are shown in Table 1.

Geological Evidence Map

Evidential map for geology was created using combination of geological factor maps of lithology, litho-contacts, faults, shear and fracture systems, quartz vein, etc. Literature consultation and available data pertaining to this particular area reveals granite and rhyolites as important hosts for hydrothermal copper, gold, fluorite, REE, mineralisation and hence, were accorded higher priority in ranking. Instances of gold are also reported from basic volcanics in the northern parts of the area which has been duly considered. Mineralisation in the study area shows close relation to faults and brittle ductile shear systems allowing the geologists to assign higher priority to these structural factors in prospectivity mapping. Proximity buffers were created for all such faults, shears, quartz veins, etc. and accorded suitable class scores for creating factor maps (Table 1, Fig.4 a-g).

Aero-magnetic Evidence Map

The first vertical derivative map (FVD) (Fig. 2) of the area has brought out a number of local and conspicuous N-S and NW-SE

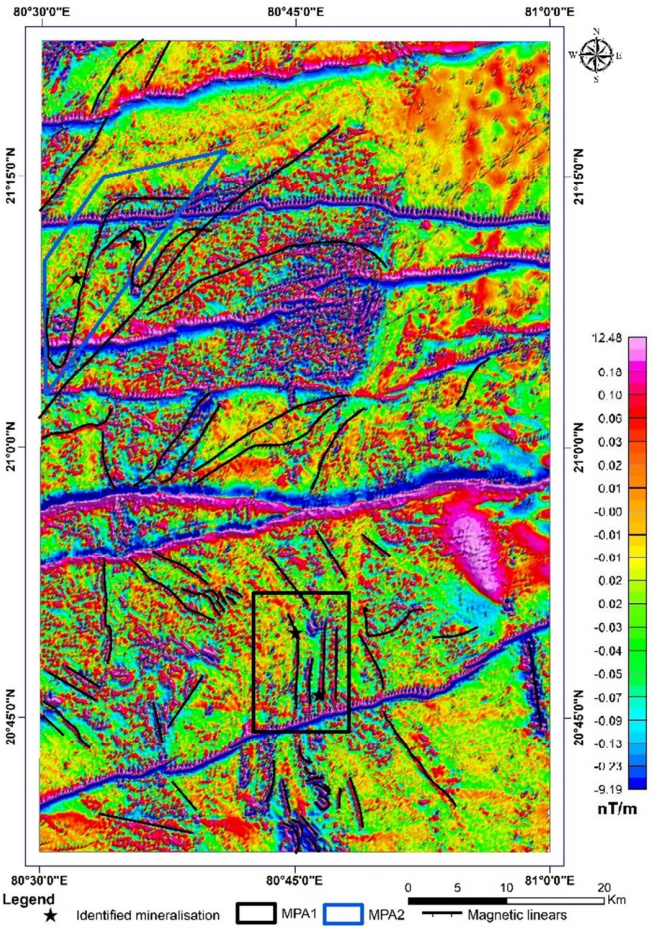

Fig.2. First vertical derivative map of the area.

trending magnetic linears present over Bijli rhyolite and Pitepani basalts in the south-western and north-western part of the area respectively. These magnetic linears, especially in the south showed close spatial relation with the brittle-ductile shear systems and hydrothermal alteration zones of secondary silicification, ferruginisation and limonitisation indicating fluid remobilisation. Since, fluids movement in general play a role in hydrothermal mineralisation, aero-magnetic evidence map has been considered crucial for favourability/potential mapping of hydrothermal minerals. Suitable scores were assigned to each proximity buffer and aeromagnetic evidence map was generated (Table 1, Fig. 4h).

Radiometric Evidence Map

Quantitative analysis of K % map reveals a number of linear potash lows in the western and south western parts of the area over rhyolites of Nandgaon Group bearing close resemblance with silicified fault zones and inferred magnetic faults. Radiometric data have been successfully utilised in demarcating potash hydrothermal alteration zones using K% radioelement map and eTh/K ratio maps (Fig.3) (Shives et al. 1997, Irvine and Smith,1990). Anomalous K % values and eTh/K low zones are indicator of faults and shear zones because increased permeability in such areas leads to remobilisation of thorium and relative potash enrichment (Hoover et al.1992). Such zones have been digitised and proximity analysis have been done to create buffers for creation of K% and eTh/K ratio factor maps (Table 1, Fig. 4 i-j). Radiometric evidence map is a combination of K% and eTh/K ratio factor maps.

Alteration Evidence Map

Alteration zones mapping reveals presence of phyllic alteration in

Table 1. Fuzzy membership values for evidential maps

Evidential class	Class score	Map Score	Evidence Class Score	Fuzzy membership	Evidential class	Class score	Map Score	Evidence ClassScore	Fuzzy membership
Geology					**Gamma ray spectrometric**				
Lithology					**Potash (K %)**				
Granite	8	8	64	6.4	Buffer 400 m	9	7	63	6.3
Rhyolite	7	8	56	5.6	Buffer 600 m	8	7	56	5.6
Mica Schist	6	8	48	4.8	Buffer 800 m	7	7	49	4.9
Basalt	5	8	40	4.0	**Thorium to potassium ratio (eTh/K low)**				
Gabbro	1	8	8	0.8	Buffer 400 m	8	7	56	5.6
Laterite	1	8	8	0.8	Buffer 600 m	7	7	49	4.9
Sandstone	1	8	8	0.8	Buffer 800 m	6	7	42	4.2
Vein Quartz					**Alteration**				
Buffer 400 m	9	9	81	8.1	Phyllic				
Buffer 800 m	8	9	72	7.2	Buffer 300 m	7	6	42	4.2
Buffer 1200 m	7	9	63	6.3	Buffer 600 m	6	6	36	3.6
Lithological Contact					Buffer 800 m	5	6	30	3.0
Buffer 400 m	9	8	72	7.2	Propylitic				
Buffer 600 m	8	8	64	6.4	Buffer 200	8	8	64	6.4
Buffer 800 m	7	8	56	5.6	Buffer 400	7	8	56	5.6
Fold					Buffer 600	6	8	48	4.8
Buffer 400 m	8	8	64	6.4	Argillic				
Buffer 800 m	7	8	56	5.6	Buffer 200	7	7	49	4.9
Buffer 1200 m	6	8	48	4.8	Buffer 400	6	7	42	5.2
Fault					Buffer 600	5	7	35	3.5
Buffer 400 m	9	9	81	8.1	**Geochemical**				
Buffer 600 m	8	9	72	7.2	**Copper dispersion pattern**				
Buffer 800 m	7	9	63	6.3	Buffer 500	9	9	81	8.1
Shear					Buffer 1000	8	9	72	7.2
Buffer 300 m	9	9	81	8.1	Buffer 1500	7	9	63	6.3
Buffer 600 m	8	9	72	7.2	**Lead dispersion pattern**				
Buffer 900 m	7	9	63	6.3	Buffer 300	8	8	64	6.4
Fracture system					Buffer 500	7	8	56	5.6
Buffer 100 m	7	7	49	4.9	Buffer 700	6	8	48	4.8
Buffer 300 m	6	7	42	4.2	**Copper dispersion pattern**				
Buffer 400 m	5	7	35	3.5	Buffer 300	7	7	49	4.9
Aeromagnetic					Buffer 600	6	7	42	4.2
Magnetic discontinuities/faults					Buffer 900	5	7	35	3.5
Buffer 500 m	9	9	81	8.1					
Buffer 800 m	8	9	72	7.2					
Buffer 1000 m	7	9	63	6.3					

the southern part of the area in close proximity of faults near village Murpar as well as over rhyolites of Nandgaon volcanics to the west of Chandidongri fault. Prominent argillic alteration which entails presence of kaolinite-alunite-pyrophyllite has been observed over north western and central part of the Dongargarh granite to the east of Chandidongri fault. Propylitic alteration which accounts for chlorite-epidote-carbonate mineral assemblage is found to occur mostly over metabasics rocks of Khairagarh Group in the north western part of the area as well as over felsic volcanics near Bhansula and Kotra in the south central part of the area. Alteration factor maps each for phyllic, argillic and propylitic alteration are created by suitable scores assignment to proximity buffers. The combination of these three factor maps forms the alteration evidence map (Table-1, Fig.4 k-m).

Geochemical Evidence Map

Elemental distribution maps reveal a variation range of Cu between 3 to 101 in ppm with a linear N-S trending anomalous copper trend over Dongargarh granite (DG) and at places over basalts of Khairagarh Group. Lead shows a concentration range of 2 to 118 ppm, showing a distinct E-W trend over central portion of the Dongargarh granite in close association with N-S trending Chandidongri shear zone. Zinc distribution map reports a value range of 30 to 116 ppm and shows an elevated concentration in the north western part over volcano sedimentary Khairagarh Group of rocks and metabasics of Nandgaon group. The enrichment patterns of these three elements are largely controlled by presence of shear and fracture systems and density of quartz veins in the area. A geochemical evidence map incorporates the factor maps for copper, lead and zinc with suitably assigned scores (Table 1, Fig.4 n-p).

Criteria for Mineral Favourability Mapping

Every mineral prediction model is based on certain assumptions that are reasonably suited and hold true in the opinion of the of the domain experts. The fuzzy modelling demonstrated here for mineral favourability mapping is based on the assumptions that (i) basic data pertaining to the lithology, structures, wall rock alteration, geochemical dispersion of pathfinder elements, etc., of the study area is available and are true and reliable (ii) the existing mineral occurrence/s are studied in detail and characterised in respect of their genesis and factors enabling mineralisation. Literature review of the area reveals that mineral occurrences in the study area indicate hydrothermal origin owing to their proximity with quartz veins, brittle-ductile shear zones, fractures and folds hinges, faults, etc. It is inferred that, the enhanced permeability in these weak zones might have facilitated movement of fluids causing wall rock alteration in the form of secondary silicification, ferruginisation, chloritization, epidotisation, etc. and

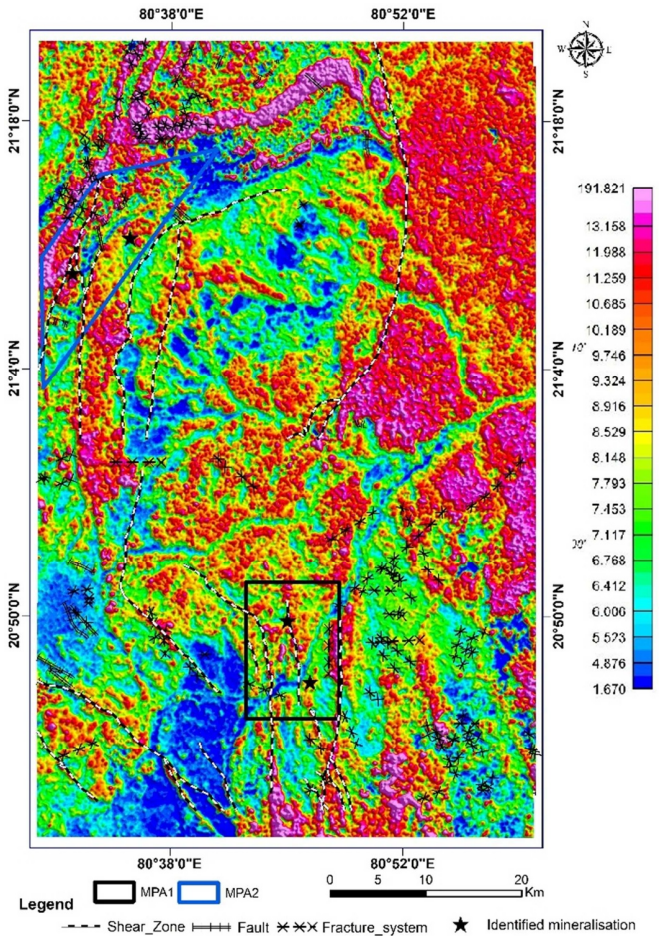

Fig.3. Radiometric eTh/K ratio map of the area.

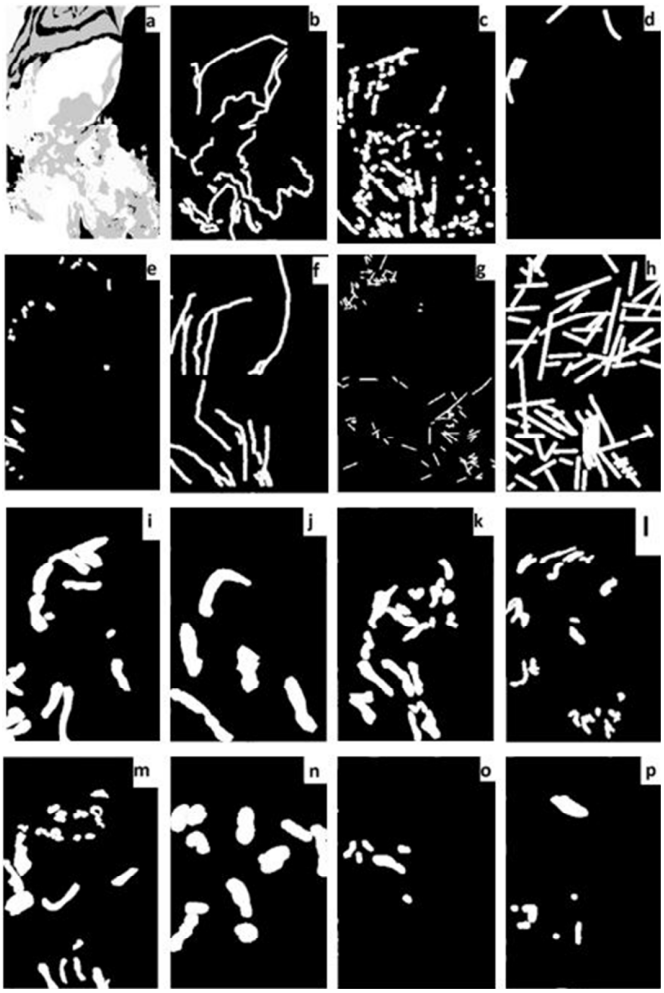

Fig.4. Factor maps for all layers of evidence.

ultimately depositing the metals in the form of pyrite, chalcopyrite, gold, REE, etc. It is therefore, pertinent to model these attributes to build a mineral prediction model i.e. mineral favourability map (MFM) suitable for this particular area. Considering a significant role of faults, shear zones, fractures, etc., map scores for faults, shear and fractures are given a score of 9 out of 10 (Table-1). Proximity buffers have been created judiciously with maximum buffer distance of 800m, 900m and 400m respectively for fault, shear and fractures depending on the fact that the faults and shear zones in the area have larger spatial extents and hence have higher area of influence as compared to the fractures systems. Faults and shear zones extracted from the magnetic data have been given high score of 9 out of 10 and buffers have been kept within comparable range of faults and shear zones (Table1). On similar lines, evidential layers have been created for potash enrichment and eTh/K low zones in radiometric data, phyllic, argillic and propylitic alteration zones deduced from remote sensing data and for dispersion pattern of pathfinder elements from geochemical data by creating buffers and assigning scores based on subjective assessment of favourability for each layer. The evidence class score have been calculated by multiplying class score and map score as shown in Table 1. On the basis of their suitability in the model, all classes in the evidential maps are ranked between 1-10 with 10 being the most favourable and 1 being the least. Score allotment of 10 is avoided in the model owing to the fact that it is highly difficult to assess that which buffer distance from a particular feature or factor is most suitable for mineralisation.

Integration of Evidence Maps

As previously mentioned, the evidential layers are spatially correlated with each other with the help of mathematical operator such as fuzzy "AND", fuzzy "OR", fuzzy algebraic "PRODUCT" and fuzzy algebraic "SUM" and fuzzy GAMMA operators using various mathematical algorithms run on GIS platform. Each of these mathematical operations result into a map with certain sets of information with respect to potential areas of mineralisation. The fuzzy OR is similar to the Boolean OR (logical union) whereby the output fuzzy membership values are controlled by the maximum values of any of the input maps, for any particular location. The fuzzy OR is defined by following equation;

$$\mu_{combination} = MAX\ (\mu_A,\ \mu_B,\ \mu_C \ldots)$$

where μ_A is the fuzzy membership value for map A at a particular location, μ_B is the fuzzy membership value for map B, and so on. The fuzzy AND operation is equivalent to a Boolean AND (logical intersection) operation on classical set values of 1 and 0. It is defined by following equation;

$$\mu_{combination} = MIN\ (\mu_A,\ \mu_B,\ \mu_C \ldots)$$

where μ_A is the fuzzy membership value for map A at a particular location, μ_B is the fuzzy membership value for map B, and so on. The fuzzy algebraic 'PRODUCT' is defined by equation;

$$\mu_{combination} = \prod_{i=1}^{n} \mu_i$$

where μ_i is the fuzzy membership value (i =1,2,3,…n). The combined fuzzy membership values tend to be small with this operator, because of the effect of multiplying several numbers less than 1. The

output is always smaller than, or equal to, the smallest contributing fuzzy membership value, and is thus "decreasive." The fuzzy algebraic SUM operator is complementary to the fuzzy algebraic product, and is defined by the following equation;

$$\mu_{combination} = 1 - \prod_{i=1}^{n} (1 - \mu_i)$$

where μ_i is the fuzzy membership value for the i-th map and i=1, 2,3,.... n maps are to be combined. The result of this operation is always larger than, or equal to the largest contributing fuzzy membership value. The effect thus is "increasive". In the current project, all the evidence layers are combined using fuzzy gamma 'γ' operator to obtain the end product i.e. mineral favourability map by utilising the following equation of Zimmermann and Zysno (1980)

$$\mu_{combination} = (\prod_{i=1}^{n} \mu_i)^{1-\gamma} (1 - \prod_{i=1}^{n} (1 - \mu_i))^{\gamma}$$

This "γ-operator" is a combination of the fuzzy algebraic product and the fuzzy algebraic sum, where 'γ' is a parameter between the range 0 and 1 and μ_i represents fuzzy membership values. In the fuzzy gamma operation, when 'γ' is 1, the combination result is the same as the fuzzy algebraic sum, and when 'γ' is 0 the combination result equals the fuzzy algebraic product. Judicious choice of 'γ' produces output values that ensures a flexible compromise between the 'increasive' tendencies of the fuzzy algebraic sum and the 'decreasive' effects of the fuzzy algebraic product. As opined by Bonham-Carter (1994) that to generate the increasing effects of fuzzy membership values in the final prediction map the gamma value needs to be above 0.8. In the current exercise, mineral favourability maps were generated by using two values of gamma operator 'γ' i.e. 0.8 and 0.9 and the results were compared. However, the mineral favourability map with 'γ' value 0.9 when validated in field, yielded positive results in the form of identification of two promising mineral potential areas which are characterised as under. It is pertinent to mention that the selection of values for fuzzy membership function and allocation of weights is subjective and end product is dynamic which may be improved at any point of time depending upon access to new technology, increased data density and field evidences. The end product so obtained is a mineral favourability map where brighter pixels indicate higher possibility of mineralisation and darker areas represent areas with lesser possibility (Fig. 5).

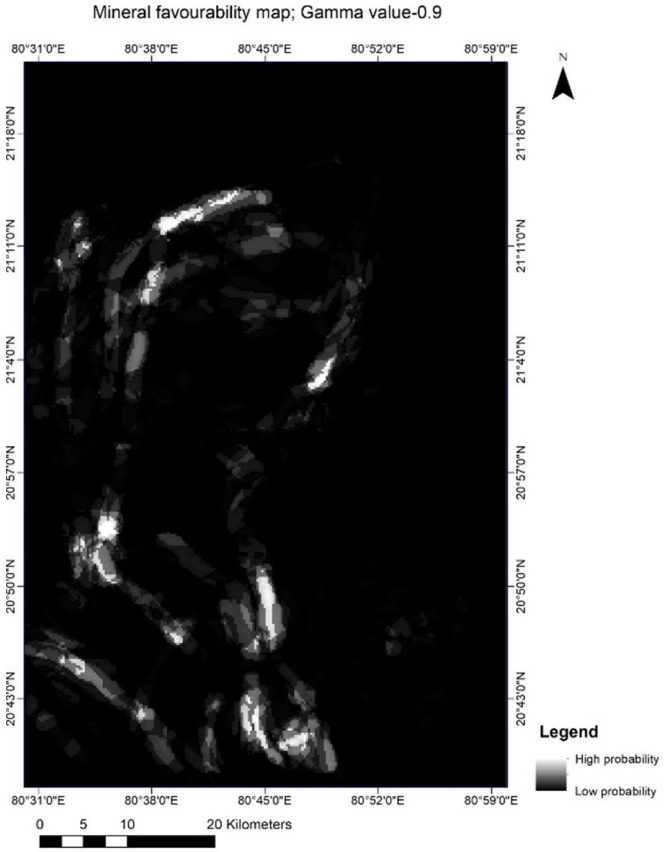

Fig.5. Mineral favourability map produced through data integration.

FIELD AND LABORATORY RESULTS

The mineral favourability map has been further examined in conjunction with litho- structural attributes and exploration data base for selection of appropriate areas for field investigation. Field evaluation of modelling output included critical appraisal of the mineral favourability areas vis a vis lithology, structural features, favourable host rocks, high strain zones, wall rock alterations, magnetic linears, evidences of sulphide mineralisation, collection of representative samples followed by petro-minerographic and geochemical probing. Synthesis of modelling outputs, field data and laboratory results has identified two mineral potential areas/zones (MPA) namely (i) Kotra-Bhansula area and (ii) Bhursatola-Khampura area

Characterisation of Identified Mineral Potential Areas

MPA-1 Kotra- Bhansula Area

This zone spreading over an area of 50-70 sq. km, is predominantly represented by dark grey coloured, massive to jointed, porphyritic felsic volcanics (Bijli rhyolite) with occasional presence of N-S and NW-SE trending mafic dykes along the joint planes. Linearly disposed, N-S oriented, brittle ductile shear zones mark significant structural entities in this zone. These shear zones are marked by topographic highs comprising of fractured and brecciated silicified zones (3-15m wide and 200-300m long). In addition to secondary silicification, iron oxide alteration, carbonatization and epidotisation are other prevalent wall rock alteration types in the area. Evidences of leaching in the form of boxworks have been documented along the shear zones. The matrix supported hydrothermal breccia constitutes randomly oriented angular clasts of quartz and host rock fragments embedded in reddish brown goethite and chlorite matrix (Fig.6a). Petrographic study and SEM EDS analysis of host rock samples shows phenocrysts of quartz and orthoclase and albite in finer groundmass largely represented by quartz and orthoclase. The host Bijli rhyolite in this MPA show variable wall rock alteration in the form of silicification, K felspathisation, epidotisation and iron oxide formation in proximity with the sheared and fractured domains. Veins of silica, iron oxide and epidote occupying the fracture planes are observed at various places (Fig.6b).

Pyrite, chalcopyrite, galena and sphalerite represent the principal sulphide mineral assemblage in the Kotra area occurring as vein fillings in association with quartz, K feldspar, barite, chlorite and calcite (Fig.6c). Disseminated grains of scheelite and cassiterite have also been observed in association with fluorite and calcite veins (Fig.6d). Additionally, scheelite is also observed to occur as inclusions within larger grains of pyrite. SEM and EPMA probing have also confirmed presence of REE bearing phases such as Nb bearing baotite, allanite, britholite, monazite and florencite in association with quartz and fluorite. Li bearing phyllosilicates such as polylithionite and zinwaldite in association with quartz, muscovite and kaolinite.

Evaluation of aero-magnetic data (FVD map) for this MPA reveals a close association of the parallel shear zones with linearly trending magnetic anomaly (Fig.2). Radially averaged power spectrum analysis of the linear anomalies reveals their absence in middle and deeper layer map, thus attesting their shallow origin and depth. Analysis of radioelement concentration maps (radiometric maps) reveals a eTh/

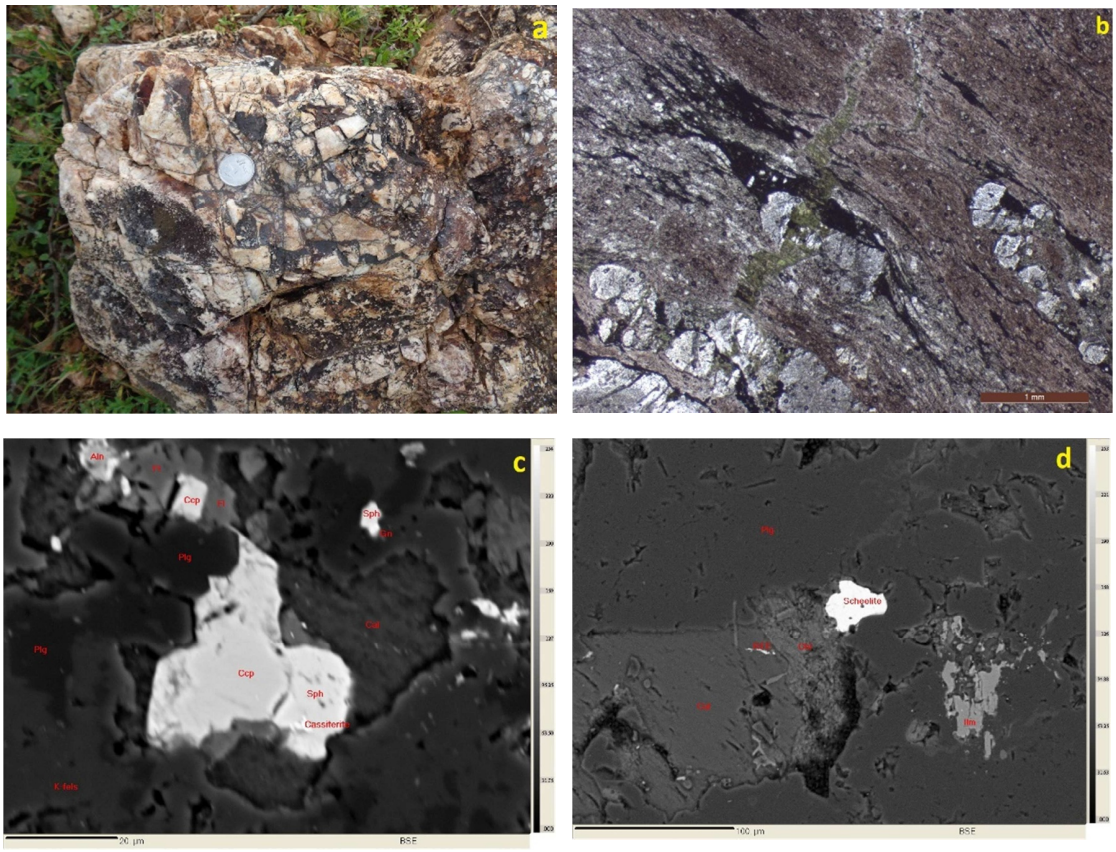

Fig.6. (a) Hydrothermal breccia with angular clasts of quartz in a matrix of goethite and chlorite. **(b)** Photomicrograph of host rhyolite from Kotra Bhansula area showing epidotisation and iron oxide alteration. **(c)** BSE image showing occurrence of chalcopyrite, sphalerite and cassiterite in sheared rhyolite in Kotra. **(d)** Occurrence of scheelite in association with calcite and chlorite in Kotra area.

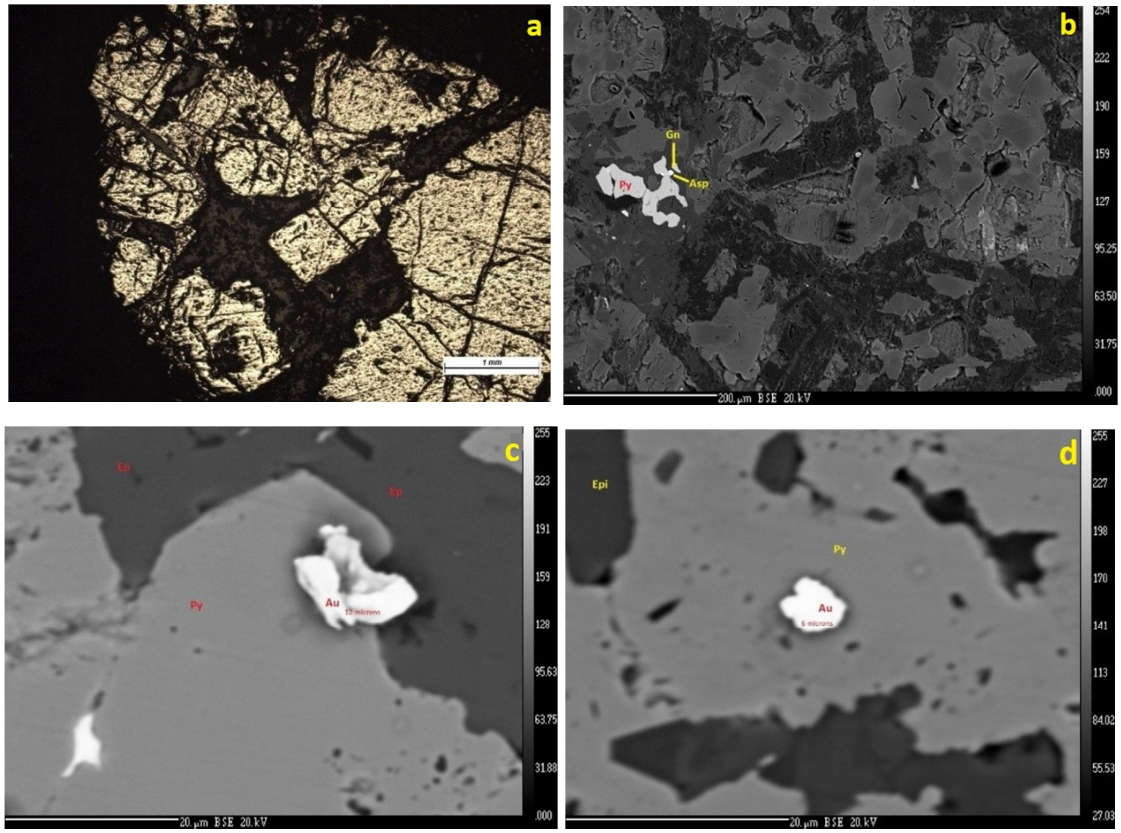

Fig.7 (a) Cataclastically deformed pyrite (Py) grains occurring in sheared and propylitically altered portions of host rock. **(b)** Pyrite, galena (Gn) and arsenopyrite (Asp) occurring in metabasalt of Bhursatola-Khampura MPA. **(c-d)** Dissemination of gold grains in propylitic mineral assemblage in the Bhursatola-Khampura MPA.

K low response over these shears representing hydrothermal alteration in this area (Fig.3).

MPA-2 Bhursatola-Khampura area

Ground characterisation of Bhursatola-Khampura MPA in the western sector of the study area, to the north of Ghortalao forest, revealed presence of patchy outcrops of fine grained metabasic rocks in a low lying flat topography. Megascopically, the rock is greenish in colour and is comprised of pyroxenes, amphiboles, plagioclase, iron oxides, etc. Vesicles filled with dark coloured minerals were also observed at some of the places. Petrography revealed that plagioclase, pyroxenes and Fe-Ti oxides form a major bulk of the constituent minerals. Calcic plagioclase feldspar occur as phenocrysts in a groundmass composed of pyroxene and amphiboles and roughly occupy 20-30 percent of the volume. Iron oxides mostly magnetite and ilmenite are present as opaque minerals. Presence of fine networks of quartz and carbonate veins within the rock demonstrates hydrothermal activity within the metabasics. Alteration in the form of epidotisation and chloritization were also recorded at places. Sulphide mineralisation is represented by a mineral assemblage of pyrite, chalcopyrite, galena and arsenopyrite. Pyrite and chalcopyrite are present in the form of chunks and disseminations within quartz and calcite veins occupying the fracture planes. Exposure of sulphides to air has led to tarnishing of sulphides and formation reddish brown spots due to oxidation. Pyrite is the most dominant sulphide followed by chalcopyrite and arsenopyrite. Pyrite is mostly equant shaped and euhedral in nature showing whitish yellow appearance occurring mostly as vein fillings and disseminations. Pyrite occurring as disseminations within host metabasic are mostly equant and euhedral, while those associated with calcite veins are cataclastically deformed (Fig.7a). Chalcopyrite is present mostly as dissemination within quartz veins intrusive into the host metabasalt. Arsenopyrite occur as inclusions in pyrites and galena (Fig.7b). Dissemination of gold grains within a size range of 3 microns to 12 microns have been found to be present as inclusion within the pyrites and in fracture planes dominated by epidote, calcite and chlorite mineral assemblage (Fig.7c-d). Analysis of the first vertical derivative (FVD) map reveal that areas of sulphide and gold mineralisation lie in close proximity with a S shaped magnetic anomaly sandwiched between two prominent E-W magnetic linears (Fig.3). It was further observed that the identified anomaly in the FVD map marks the contact between the crystalline Nandgaon volcanics and sediments of Khairagarh Group.

DISCUSSION AND CONCLUSION

A knowledge based mineral favourability mapping commence with collection and collation of geoscience data and determination of proxies of mineralisation based on ground geological knowledge of the type of mineral system targeted. A number of data sets in respect of geology, airborne geophysics, soil geochemical dispersion values and remote sensing were utilised to execute the current exercise of data integration. Knowledge-based criteria extracted from these datasets included prospective lithounits, density and proximity with faults, shear, fracture system, magnetic linears, alteration zones, favourable radiometric indicators, etc. The success of a knowledge driven method relies heavily upon the quality and interpretation of the data, understanding and expertise of the team in respect of the targeted mineral system and a judicious use of weights for each individual evidence layers. A meagre amount of bias in data and weight assignment is still possible which makes the model vulnerable and may yield false anomalies in terms of potential target areas. This has been minimised in the current work with the help of a collective approach of experts from different domains and by critical exchange of ideas and knowledge amongst them. The mineral favourability map generated in this exercise of data integration is a general mineral favourability index which gives a general indication of mineral potential. Favourability areas for mineralisation account for about 10-15 % of the total area resulting into significant decrease in area to be scanned during field work. However, critical evaluation of the mineral favourability areas during field investigation helped in identification of two mineral potential areas (MPAs). MPA in Kotra-Bhansula area indicate presence of silicified zones with variable degree of chlorite, iron oxide and epidote alteration within meta acid volcanics in close spatial proximity with shear and fracture systems. Petro-minerographic probing of the representative samples collected from the Kotra area reveals presence of pyrite, chalcopyrite, cassiterite and scheelite mineralisation in the sheared rhyolites. A close spatial association between the linear magnetic highs, silicification, iron oxide alteration and mineralisation is a unique character in this MPA in the southern sector and may serve as proximator in further exploration. On the other hand, the second MPA near Bhursatola-Khampura area offers promise with respect to metabasalt hosted copper and gold mineralisation in the propylitically altered zones. It is felt that, in both the mineral potential areas, although the near surface samples do no indicate very encouraging values, however, shallow to medium depth of linear magnetic anomalies corroborating with shear zones indicate possibility of finding metalliferous zones at depth. Consequently, sub-surface probing using other geophysical techniques and or drilling is warranted in these zones. It can be held that the objective of this paper have been met in a way that a recently acquired high resolution airborne geophysical data has been utilised in conjunction with legacy geoscience data to produce a mineral favourability map. Ideally, the favourability/prospectivity map so produced is not an absolute target map but a broader categorisation of favourable and unfavourable areas for initiating G-4 stage or reconnaissance exploratory activities.

Acknowledgement: The authors thank Dr. Bijay Kumar Sahu, former Deputy Director General and HoD, Remote Sensing and Aerial Survey, Geological Survey of India, Bangalore for his valuable contribution in interpretation of aero-geophysical data, mineral prediction modelling and for his guidance during the field investigation.

References

Ahmad, T., Wanjari, N., Kaulina, T.V., Mishra, M.K and Nitkina, E.A. (2008) Geochemical and isotopic characteristics of the Amgaon gneissic complex, Central Indian Shield: Constraints on Precambrian crustal evolution. In: Proc. Int. Symp. 'Geoscience Resources and Environments of Asian Terranes (GREAT-2008), 4th IGCP 516, and 5 APSEG;' November 24-26, 2008, Bangkok, Thailand.

Bleeker, W. (2003) The late Archaean record: A puzzle in ca. 35 pieces. Lithos, v.71(2-4), pp.99-134.

Bonham-Carter, G.F. (1994) Geographic information systems for geoscientists-modeling with GIS. Comput. Methods Geosci., v.13, pp.398

Carranza, E., van Ruitenbeek, F., Hecker, C., van der Meijde, M., and van der Meer, F. (2008) Knowledge-guided data driven evidential belief modeling of mineral prospectivity in Cabo de Gata, SE Spain. Internat. Jour. Appl. Earth Observ.Geoinform., v.10, pp.374–387.

Carranza, E.J.M. (2009) Geochemical Anomaly and mineral prospectivity mapping in GIS. *In:* Handbook of Exploration & Environmental Geochemistry; Elsevier: Amsterdam, The Netherlands, Volume 11, p.368.

Dubois, D., Hajek, P. and Prade, H. (1999) Knowledge-driven versus data-driven logics. Jour. Log. Lang. Inf. v.9, pp.65–89.

Feltrin, L. (2008) Predictive modelling of prospectivity for Pb–Zn deposits in the Lawn Hill Region, Queensland, Australia. Ore Geol. Rev., v.34, pp.399–427.

Hoover, D.B., Heran, W.D. and Hill, P.L. (1992) The geophysical expression of selected mineral deposit models. USGS. Open-File report 92–557, 129p.

Irvine, R.J. and Smith, M.J. (1990) Geophysical exploration for epithermal gold deposits. Jour. Geochem. Explor., v.36, pp.375–412.

Krishnamurthy, P., Sinha, D.K., Rai, A.K., Seth, D.K. and Singh, S.N. (1990) Magmatic rocks of the Dongargarh Supergroup, Central India – Their Petrological evolution and Implications on Metallogeny. Geol. Surv. India

Spec. Publ., v.28, pp.303–319.
Naqvi, S.M. (2005) Geology and Evolution of the Indian Plate. Capital Publishing Co., New Delhi, 448p.
Pan, G. and Harris, D. (2000) Information Synthesis for Mineral Exploration; Oxford University Press, New York, NY, USA
Porwal, A., Carranza, E.J.M., Hale, M. (2003) Knowledge-driven and data-driven fuzzy models for predictive mineral potential mapping. Nat. Resour. Res., v.12, pp.1–25.
Ramakrishnan, M. and Vaidyanadhan, R. (2010) Geology of India, Geol. Soc. India, Bangalore, v.1, 558p.
Sarkar, S.N. (1957–58) Stratigraphy and tectonics of the Dongargarh System, a new system in the Precambrians of Bhandara-Durg-Balaghat area, Bombay and Madhya Pradesh; Jour. Sci. Engg. Res., IIT, Kharagpur, India, v.1, pp.237–268, v.2, pp.145–160.
Sarkar, S.N., Sarkar, S.S. and Ray, S.L. (1994) Geochemistry and genesis of the Dongargarh Supergroup Precambrian rocks in Bhandara-Durg Region, Central India. Indian Jour. Earth Sci., v.21, pp.117–126.
Sensarma, S. and Mukhopadhyay, D. (2003) New Insight on the stratigraphy and volcanic history of the Dongargarh Belt, Central India. Gondwana Geol. Mag. Spec. Vol. 7, pp.129–136.
Shives, R.B.K., Charbonneau, B.K., Ford, K.L. (1997) The detection of potassic alteration by gamma ray recognition of alteration related to mineralization, in: Exploration 97, Fourth Decennial Intern. Conf. Mineral Exploration (Toronto, Canada), pp.345–353.
Zadeh, L.A. (1965) Fuzzy sets. IEEE Information and Control, v.8(3), pp.338–353.
Zimmermann, H.-J. (1991). Fuzzy set theory – And its applications. Dordrecht: Kluwer Academic, 2nd edition, 399p.
Zimmermann, H.-J. and Zysno, P. (1980) Latent connectives in human decision making. Fuzzy Sets and Systems, v.4, pp.37–51.